Neuroscience 329 (2016) 349–362

WHITE MATTER AND TASK-SWITCHING IN YOUNG ADULTS: A DIFFUSION TENSOR IMAGING STUDY

ANTONINO VALLESI, [a,b]* **ELEONORA MASTRORILLI,** [a,c] **FRANCESCO CAUSIN,** [d] **DOMENICO D'AVELLA** [a,b] **AND ALESSANDRA BERTOLDO** [c]

[a] *Department of Neuroscience, University of Padova, Italy*

[b] *Centro di Neuroscienze Cognitive, University of Padova, Italy*

[c] *Department of Information Engineering, University of Padova, Italy*

[d] *Neuroradiology Unit, Azienda Ospedaliera di Padova, Italy*

Abstract—The capacity to flexibly switch between different task rules has been previously associated with distributed fronto-parietal networks, predominantly in the left hemisphere for phasic switching sub-processes, and in the right hemisphere for more tonic aspects of task-switching, such as rule maintenance and management. It is thus likely that the white matter (WM) connectivity between these regions is critical in sustaining the flexibility required by task-switching. This study examined the relationship between WM microstructure in young adults and task-switching performance in different paradigms: classical shape-color, spatial and grammatical tasks. The main results showed an association between WM integrity in anterior portions of the corpus callosum (genu and body) and a sustained measure of task-switching performance. In particular, a higher fractional anisotropy and a lower radial diffusivity in these WM regions were associated with smaller mixing costs both in the spatial task-switching paradigm and in the shape-color one, as confirmed by a conjunction analysis. No association was found with behavioral measures obtained in the grammatical task-switching paradigm. The switch costs, a measure of phasic switching processes, were not correlated with WM microstructure in any task. This study shows that a more efficient inter-hemispheric connectivity within the frontal lobes favors sustained task-switching processes, especially with task contexts embedding non-verbal components.

Key words: task-switching, fractional anisotropy, radial diffusivity, executive functions, corpus callosum, FSL.

INTRODUCTION

The capacity to switch from one rule to another in order to accomplish internal or external goals is an important executive function at the basis of cognitive flexibility. This capacity has been experimentally investigated through the task-switching paradigm (e.g., Rogers and Monsell, 1995). Performance on this paradigm involves two partially dissociable control processes: transient (or local) control and sustained (or global) control (Braver et al., 2003). These processes are captured by two different behavioral effects: (a) switch costs, that is, performance difference between trials in which the rule changes and trials in which it is repeated in mixed task blocks; and (b) mixing costs, that is, performance difference between repetition conditions during mixed-task blocks and single task conditions in pure blocks, respectively.

Neuroimaging studies have characterized distributed networks of fronto-parietal and striatal regions during task-switching (Dove et al., 2000; Brass and von Cramon, 2004; Badre and Wagner, 2006; Jamadar et al., 2015). The key domain- and rule-independent task-switching-related cognitive control processes have been mainly located in fronto-parietal networks of the left hemisphere (Kim et al., 2011; Jamadar et al., 2015; Vallesi et al., 2015; cf. De Baene et al., 2012, for an alternative view based on adaptation mechanisms).

However, additional right lateral prefrontal recruitment has been observed for task-switching paradigms with non-verbal (i.e., spatial) rules (e.g., Vallesi et al., 2015), compatibly with what happens in other high-level cognitive domains such as inductive reasoning (e.g., Babcock and Vallesi, 2015). Moreover, previous neuroimaging evidence (Braver et al., 2003) showed that right anterior prefrontal regions were activated in mixed (vs. single-task) blocks, which require the capacity to maintain and manage task-rules over-time (also see Ambrosini and Vallesi, 2016 for converging resting-state electroencephalographic evidence).

Thus, given the distributed nature of the brain circuits involved in task switching (Dove et al., 2000; Kim et al., 2012; Jamadar et al., 2015), white matter (WM) connectivity studies with Diffusion Tensor Imaging (DTI) are especially important to fully characterize the neural underpinning of these functions.

DTI provides an *in vivo* estimate of WM microstructure by measuring the degree and orientation of preferential diffusion of water molecules in neural tissue (Basser and Pierpaoli, 1996; Beaulieu, 2002; Le Bihan, 2003).

*Correspondence to: Department of Neuroscience, University of Padova, Via Giustiniani, 5, 35128 Padova, Italy. Tel: +39-049-821-4450; fax: +39-049-821-8988.
E-mail address: antonino.vallesi@unipd.it (A. Vallesi).

Abbreviations: DTI, Diffusion Tensor Imaging; EPI, echo-planar image; FA, fractional anisotropy; fMRI, functional magnetic resonance imaging; MNI, Montreal Neurological Institute; RD, radial diffusivity; ROIs, Regions Of Interest; RTs, response times; SD, standard deviation; WM, white matter.

http://dx.doi.org/10.1016/j.neuroscience.2016.05.026

Several scalar indices are extracted from this model to summarize this information at the voxel level (Alexander et al., 2007). Fractional anisotropy (FA) is the most commonly used value, that describes the fraction of the tensor related to anisotropic water diffusion, while radial diffusivity (RD) describes the degree of water dispersion in the plane perpendicular to the main diffusivity direction. Higher FA and lower RD values are related to increased WM integrity and fiber organization (Pfefferbaum et al., 2000; O'Sullivan et al., 2001).

A previous multimodal neuroimaging study (Gold et al., 2010) using a number-letter task-switching paradigm already tested the relationship between WM integrity in twelve pre-selected Regions Of Interest (ROIs) and global switching costs (i.e., RT difference between mixed vs. single task conditions) in twenty younger and twenty older adults. In general, global mixing costs were negatively correlated with FA bilaterally in the superior longitudinal fasciculus and pericallosal frontal regions, suggesting that the integrity of WM tracts connecting prefrontal regions or fronto-parietal regions is associated with better task-switching (i.e., lower global switching costs). However, when considering the younger participants alone, only the WM-behavior correlation with the left superior longitudinal fasciculus survived.

Another recent DTI study on 10–16-year-old adolescents (Seghete et al., 2013) found a positive correlation between FA in superior corona radiata and precentral gyrus and global task-switching performance, regardless of age, whereas an association between FA in the anterior corona radiata and task-switching was present only in interaction with age.

An important aim of the present study was to investigate whether the integrity of some WM tracts is associated to task-switching performance based on, or independently of, the specific nature of the task-switching rules employed. Therefore, as a novel contribution to the still scant literature on the association between DTI and task-switching performance in young adults (see Gold et al., 2010; Seghete et al., 2013; Treit et al., 2014, for developmentally oriented studies), rather than focusing on a single task-switching paradigm, we operationalized the task-switching construct with three different paradigms performed by the same individuals, with different degrees of verbal and non-verbal demands, and correlated the performance measures of task-switching efficiency on all these paradigms with WM integrity measures, both separately and by means of conjunction analyses across the paradigms which showed significant associations. The goal of a cross-paradigm replication is not only motivated by the theoretical question regarding the existence of common brain mechanisms underlying cognitive flexibility, but should also be seen as a methodological attempt to better characterize structural brain-behavior correlations, a field in which it is hard to replicate results even within the same experimental paradigms (Boekel et al., 2015).

Preliminary analyses of our data did not show any reliable relationship between WM integrity and phasic task-switching costs (RT difference between switch and repeat trials). This might be due to the fact that similar neural and cognitive mechanisms might be implicated in both switch ad repeat trials, although at a different level, especially with equal probability of occurrence of the two trial types (Braver et al., 2003; Crone et al., 2006; Ruge et al., 2013). Similar null results between switch cost measures and DTI have been reported in a study with children aged 7–16 years (Treit et al., 2014). Therefore, we will report our results on mixing costs, classically calculated as the performance difference between repeat trials and single-task trials, excluding switch trials (cf., Gold et al., 2010; Seghete et al., 2013). Mixing costs are believed to indicate the active and sustained maintenance and coordination of multiple task rules, functions that have been dissociated from the phasic processing differences involved in switch vs. repeat conditions behaviorally (Rubin and Meiran, 2005), neurophysiologically (Wylie et al., 2009; Ambrosini and Vallesi, 2016) and with functional magnetic resonance imaging (fMRI) (Braver et al., 2003; Wang et al., 2009). Finally, we adopted a whole-brain approach to characterize the role of all main WM fibers, while avoiding any a priori choice of ROIs that could possibly bias the results by leaving some of the main tracts unexplored.

Our main original expectations included a role of (i) the (left) superior longitudinal fasciculus in general task-switching performance, as previously reported in the DTI study by Gold and colleagues (2010), and as expected from the general involvement of left fronto-parietal regions in fMRI studies on task-switching (e.g., Kim et al., 2011; Vallesi et al., 2015), and (ii) peri-callosal cross-hemispheric anterior fiber tracts connecting homologous prefrontal regions in supporting better task-switching performance, in terms of mixing costs (Braver et al., 2003), especially when obtained in tasks with embedded non-verbal components (Vallesi et al., 2015).

EXPERIMENTAL PROCEDURES

Participants

Thirty-eight university students voluntarily took part in the experiment. We used a sample size that was nearly double with respect to that of healthy young adults tested in previous DTI work on task switching (Gold et al., 2010), as an attempt to increase statistical power, especially considering that this population shows low inter-subject variability in WM structure.

All participants gave their written informed consent prior to recruitment. They were reimbursed 25 euros for their time. All had normal or corrected-to-normal visual acuity, reported having normal color vision and no history of any neurologic/psychiatric disease. The study was approved by the Bioethical Committee of the Azienda Ospedaliera di Padova. Three participants were excluded from the analyses because of incomplete data or poor data quality. The final number of included participants was 35. All of them were right-handed (which was an inclusion criterion), as assessed with the Edinburgh Handedness Inventory (Oldfield, 1971). The average score at this test was 84.1, with a range of 45–100, over a possible total range between −100 and

100 (where negative values indicate left-handedness). There were 26 females and 9 males and their mean age was 22.5 years (range: 21–29 years).

General procedure

For each participant, testing took place in three separate sessions in different days (see next paragraph) with the following administration order: (1) the verbal and spatial task-switching paradigms; (2) the shape-color task-switching paradigm; (3) the MRI session including DTI data acquisition. The order of administration of the three sessions was fixed for all participants to minimize any error due to participant by order interaction (Miyake et al., 2000); however, during the first session, the verbal and spatial task-switching paradigms were administered in randomized order. In the second session, participants performed additional behavioral tasks investigating different executive functions, whose results will be reported elsewhere.

Behavioral tasks and procedure

The behavioral session was performed outside the MRI scanner before neuroimaging data acquisition (always within less than 3 months, range: 1–11 weeks, mostly depending on MRI time-slot availability). In each of the three task-switching paradigms, participants were requested to perform two different subtasks in which they categorized the stimuli according to different task-relevant characteristics. We shall briefly describe the paradigms below.

Shape-color paradigm. Stimuli were hearts or stars (either red or blue) presented on a white background. On each trial participants were asked to respond to either the color or the shape of the stimulus. The task rule to be applied on each trial was indicated by a visual cue located above the stimulus. To limit the use of verbal information, symbolic cues were used three colored rectangles (purple, orange and yellow) arranged horizontally for the color rule, and three black shapes (triangle, circle and square) arranged horizontally for the shape rule. Participants were required to make a choice response to each trial by pressing either the left or right arrow buttons of a keyboard with their right index or ring finger, respectively to respond to either the color or the shape of the stimulus. The four possible response-to-button mappings were counterbalanced across participants. Trials began with a fixation cross presented for 1500 ms followed by cue presentation. After a cue-to-target interval of 100 ms, the stimulus was presented in the center of the screen below the cue. Participant's response ended the trial. Incorrect responses were followed by a 100-ms beep. Participants completed five blocks of trials which formed a sandwich design. Blocks 1, 2, 4, and 5 were single-task blocks in which only one task (color or shape) was presented for the entire block, being the specific assignment counterbalanced across participants. The single-task blocks each consisted of 6 practice trials and 24 experimental trials. Block 3 was a mixed-task block with half of the trials requiring a color judgment and the other half a shape judgment. This block included 10 practice trials followed by 192 experimental trials with a short pause after 96 trials. The number of repeat and switch trials was equal.

Spatial and verbal task-switching paradigms. These were modified versions of the ones reported in a recent fMRI study (Vallesi et al., 2015). Stimuli were composed by 18 proper nouns, divided into 9 proper female nouns and 9 proper male nouns, and 18 common nouns, divided into 9 common female nouns and 9 common male nouns. All words were created by adding a 3-D effect and a 3-D rotation to manipulate their spatial configuration. Specifically, each word could assume either a clockwise or an anti-clockwise rotation (i.e., roll) and an upward or a downward rotation (i.e., pitch). Each word could be filled with one of four colors: red, blue, green or brown. The red and blue colors were associated with the task-switching condition (see below for further details), whereas the green and brown colors were used for the single-task condition. Only in the former case, the colors signaled the task to be performed. In the latter case, the colors also changed from trial to trial in order to keep the perceptual characteristics of the stimuli similar across conditions, but participants were instructed to ignore them.

In the verbal single-task session, there were two types of subtasks that participants performed separately. The gender-type subtask required pressing the "F" key on the computer keyboard with the index finger of the left hand if the word was a female noun and the "K" key with the index finger of the right hand if the word referred to a male noun. In the name-type subtask, participants had to press the "F" key for a proper name and the "K" key for a common name. The assignment of categories to response keys was counterbalanced across participants. In the verbal task-switching condition, the color of the word instructed participants about the specific subtask they had to perform on any given trial. The blue color was associated with the name-type subtask in which participants had to decide whether the word referred to a proper name or to a common name. The red color instead signaled the gender-type subtask in which the decision regarded the female/male status of the word. The response keys were the same as those used for the verbal single-task conditions. As reported above, the word colors also changed randomly between brown and green in the single-task condition but in that case they had no rules meaning for the task.

The spatial-task session was similar to the verbal one and was implemented on exactly the same word stimuli. The spatial single-subtasks comprised a roll-type subtask in which participants had to classify the words according to their roll rotation (i.e., clockwise or anti-clockwise) and a pitch-type subtask in which they had to respond to the pitch rotation (i.e., upward or downward). In the task-switching condition, when the color was blue the task was to decide whether the word was rotated clockwise or anti-clockwise, whereas when the color

was red the task was to decide whether the word was rotated upward or downward.

Half of the participants started with the verbal-task session, whereas the other half started with the spatial-task one. Each session comprised 2 single-task blocks and 4 task-switching blocks made by 32 trials each. Repeat and switch trials were presented in a pseudo-random order to guarantee roughly the same number of trials per block. Before the first and the third task-switching blocks were presented, participants performed a single-subtask according to the following order: single-task 1, task-switching 1, single-task 2, task-switching 2, 3 and 4. The first task-switching block was also preceded by 5 warm-up trials that allowed participants to refresh the corresponding stimulus–response mapping.

A trial started with the presentation of a 400 ms gray blank screen, which contained a gray frame lighter than the background color. After that time elapsed, the word stimulus, which was embedded into the frame, was displayed for 2000 ms. Participants had to categorize the word according to the specific task instructions of each condition as outlined below. Following the period of 2000 ms, the next trial began after a 1400-ms inter-trial blank interval. Before the real test, participants practiced both verbal and spatial tasks. Each practice block comprised 10 trials. Participants received a feedback message (the Italian word for "wrong" displayed in red or the Italian word for "Well done" in blue) after response on each trial for a duration of 1500 ms. In order to allow participants to fully process either the verbal or the spatial features of the words, in the practice session only stimulus presentation lasted until a button-press response was detected.

MRI acquisition

MRI data were collected on a 3T Ingenia Philips whole-body MRI scanner, using a 32-channel head array coil, at the Neuroradiology Unit, Azienda Ospedaliera di Padova. Apposite cushioning was used to minimize head movements. Several types of image sequences were collected for each participant, including a T1-weighted sequence, four fMRI blocks of whole-head $T2^*$-weighted echo-planar image (EPI) sequences concomitant with the administration of different cognitive tasks, whose results were reported elsewhere (Vallesi et al., 2015), and finally diffusion tensor images for estimation of FA. DTI used an inversion recovery EPI sequence (Repetition Time, TR: 9730 ms; Echo Time, TE: 91 ms; Flip Angle: 90°; Field of View, FOV: 224 × 224, image matrix: 112 × 112, 6 signal averages, 65 axial slices of 2 mm thick, with no inter-slice gap), covering the whole cerebrum. Diffusion was measured along 32 directions (b-value = 800 s/mm^2), and three images with no diffusion weighting were acquired and averaged to obtain baseline image with a stronger signal to noise ratio. Twenty-nine of the participants reported here overlapped with those of another fMRI work using adapted versions of two of the task-switching paradigms reported here (Vallesi et al., 2015). However, the behavioral data used here were not the same since, as already stated, they were all acquired outside the scanner a few days/weeks before the MRI session, in order to increase both the ecological validity (see Hommel et al., 2012; Ruge et al., 2013) and the homogeneity of the acquisition settings among the different paradigms.

Behavioral data analysis

Response times (RTs) from incorrect responses were discarded. Trials with RTs shorter than 100 ms, were treated as guesses and also discarded. Median accuracy was greater than 88% in all the conditions of all the task-switching paradigms. Since the distributions of the RTs were skewed and/or kurtotic, we log-transformed RTs to improve normality. Moreover, to obtain measures of central tendency that were as robust as possible against aberrant observations, we applied an estimation procedure that is robust to non-normality and sample size (Rousseeuw and Verboven, 2002). For each participant and task condition, an M-estimator of location was computed with logistic psi-function and median absolute deviation as the auxiliary scale estimate, as implemented by the mloclogist and madc functions in the LIBRA Matlab library (Verboven and Hubert, 2010). It should be noted, however, that the values obtained with the M-estimator approach and a more classical data trimming method (mean ± 2 SD) were highly correlated for all the conditions (mean correlation r = .996).

Next, for each of the three task-switching paradigms, we calculated the switching cost as the difference between the M-estimator of location for switch trials and that for repeat trials. Similarly, we computed the mixing cost as the difference between the M-estimator of location for repeat trials and that for single-task trials. After these transformations, the variables measuring switching and mixing costs for the three task-switching paradigms showed acceptable skewness and kurtosis (respectively, mean = .13 and −.17; range = −.50 to .44 and −.79 to 23).

The statistical significance of both the switching and mixing costs for each of the three task-switching paradigms was assessed by means of one-sample t-tests. The Cohen's d was used as the measure of the effect size (Cohen, 1977).

We also performed a within-subject 3 × 3 ANOVA, to compare log-transformed RTs on the three tasks (shape-color, spatial, verbal) for the three conditions (single-task, repeat, switch) more directly. Accuracy data, separately for each condition and pair of tasks, were analyzed through non-parametric Wilcoxon Matched Pairs tests.

DTI data analysis

Preprocessing and analysis of diffusion-weighted images was carried out using FSL software (http://www.fmrib.ox.ac.uk/fsl). First, DTI images (available as NIfTI files) were brain-extracted using BET (Smith, 2002) and specific binary masks were created. Subject images were corrected for motion and eddy current prior to analysis using FMRIB's Diffusion Toolbox (FDT), setting the non-weighted average image as reference. Next, the diffusion tensor model was fitted to the raw diffusion data and the

diffusion tensor matrix was estimated for each voxel. Subsequently, three eigenvectors and their respective eigenvalues were computed from the diffusion tensor matrix, and FA and RD images were created using the eigenvalue estimates. FA and RD are scalar indices summarizing the overall diffusivity properties of the voxel.

To improve generalizability of our results across subjects, voxel-wise statistical analysis of the FA data was carried out using Tract-Based Spatial Statistics (TBSS, Smith et al., 2006). All subjects' FA data were aligned into a common space using the nonlinear registration tool FNIRT (Andersson et al., 2007a,b), which uses a b-spline representation of the registration warp field (Rueckert et al., 1999). The pre-defined target chosen for alignment is the FMRIB58_FA standard space FA template, followed by affine transformation of all images into MNI152 standard space. Next, the mean FA image was created and thinned to create a mean FA skeleton, which represents the centers of all tracts common to the group. This skeleton was then thresholded at an FA value of 0.3 in order to minimize partial volume effects after warping across subjects. Each subject's aligned FA data were then projected onto this skeleton in order to account for possible residual misalignments and the resulting data were fed into voxel-wise cross-subject statistics. To examine RD images as well, they were also affine aligned to standard space, the nonlinear registration parameters determined by FNIRT were applied to these maps, and they were merged and projected onto the FA-derived WM skeleton to perform statistical comparisons. We preferred RD over mean diffusivity and axial diffusivity for the following reasons: mean diffusivity is less sensible to discriminate gray matter from WM and a previous study already showed that it is not associated with task-switching performance (Seghete et al., 2013), while axial diffusivity is more suitable for pathologic conditions (see Feldman et al., 2010; Alexander et al., 2012).

Voxel-wise statistics used a General Linear Model (GLM) approach to test for positive and negative correlations between FA, RD, and each cognitive score in order to directly examine the relationship between DTI-relevant measures and task-switching performance. As a side note, we recall that a negative correlation indicates that better performance (lower switching and mixing costs) was associated with higher FA values. Age was not included as a covariate in correlation analysis, as all participants were selected to belong to a narrow age range, usually considered homogeneous in similar studies (e.g., Zhu et al., 2014). Threshold-Free Cluster Enhancement (TFCE) correction (Smith and Nichols, 2009) was used to correct voxel-wise statistical results for multiple comparisons; significance level was set to be $\alpha = 5\%$, two-tailed. The local maxima within each significant cluster were identified by means of the cluster tool in FSL, with the -olmax option on. Anatomical locations of each significant cluster were identified using Montreal Neurological Institute (MNI) coordinates on the International Consortium Brain Mapping-DTI WM label atlas, while the probability of the belonging tract were defined using the Johns Hopkins University WM tractography atlas.

To ensure our analysis robustness, we performed a separate analysis for FA and RD correlation respectively. However, since there was a high overlap of the areas found to show significant correlation, we decided to retain only those voxels showing both a significant negative correlation with FA and a positive correlation with RD for each of our cognitive indexes. In this way we ensured to consider voxels clearly showing a significant relation of WM diffusion properties with the scores obtained when performing the tasks. In order to investigate the anatomical location of surviving voxels and their probability to belong to some well-known tracts, we performed a cluster identification analysis using the provided FSL function.

Preliminary analyses showed that switching costs in each of the three task-switching paradigms did not correlate with any cluster, according to the selected inclusion criteria and were therefore not considered further. Therefore, in the subsequently reported analyses, we only focus on mixing costs.

After the computation of simple correlations, a conjunction analysis was carried out, in order to look for overlapping WM regions which showed significant correlations with our mixing costs in at least two of the three behavioral tasks, that is, the spatial paradigm and the shape-color one. Again, we looked for overlapping regions found to show significant correlations in both FA and RD measures. A lower limit of 10 contiguous voxels was set in order to consider a cluster significant, thus withdrawing all clusters being so small to be possibly related to noise or chance.

RESULTS

Behavioral results

Raw RT data are reported in Table 1. The analysis of participants' behavioral performance (natural log-transformed RTs) revealed a classic pattern of results, with strong switching costs (for the shape-color, spatial and verbal paradigms, respectively, M = .2, .24, .19; $t(34)$ = 8.75, 14.84, 9.93, d = 1.48, 2.51, 1.68, all ps < .0001) and mixing costs (respectively, M = .54, .24, .31; $t(34)$ = 24.18, 10.24, 14.75, d = 4.09, 1.73, 2.49, all ps < .0001).

To appreciate possible task-specific differences in behavioral performance, we also compared log-RTs across tasks through a 3×3 ANOVA. This analysis showed main effects of task and conditions and their interaction. The main effect of condition [$F(2, 68) = 706.1$, $p < .0001$] confirmed the above-mentioned task-specific analyses, by showing the presence of significant mixing costs (repeat-single task difference, Tukey's $p < .001$) and switching costs (switch-repeat difference, Tukey's $p < .001$). The task main effect [$F(2, 68) = 43.2$, $p < .00001$] was due to RTs being significantly different across tasks (verbal > spatial > shape-color; for all comparisons, Tukey's $p < .001$). Finally, the task by condition interaction [$F(4, 136) = 64.195$, $p < .0001$] was due to the differences between tasks being most pronounced in

Table 1. Mean raw RTs (in ms) and percentage of accurate trials, together with their standard deviation (SD), for each condition of each task-switching paradigm. Mean switching costs and mixing costs for both speed and accuracy measures (together with their standard deviations) are also shown. Please note that RTs were log-transformed for the statistical analyses

	Mean (ms)	SD	Percent correct	SD
Shape-color				
Single	495	76	97.9	2.1
Repeat	863	191	96.3	2.3
Switch	1058	240	93.4	4.1
Switching cost	188	163	2.9	3.5
Mixing cost	423	145	1.6	3.0
Spatial				
Single	731	128	94.0	6.8
Repeat	921	158	93.4	5.2
Switch	1155	198	87.8	7.3
Switching cost	234	92	5.6	6.7
Mixing cost	190	113	0.6	7.4
Verbal (not included in the reported DTI analyses because of null effects)				
Single	768	117	95.8	5.5
Repeat	1038	141	93.4	4.2
Switch	1227	132	87.0	7.7
Switching cost	190	109	6.3	1.6
Mixing cost	270	114	5.8	3.0

the single task condition, in which RTs for the shape-color task were particularly fast. To confirm this, planned comparisons showed that the difference between the shape-color and the other two tasks was greater for the single task condition than for any of the other two conditions (for both, $p < .00001$).

We also ran similar comparisons with accuracy data by means of non-parametric Wilcoxon tests. These analyses revealed that, in the single-task condition, accuracy was lower for the spatial task than for the shape-color one ($Z = 2.90$, $p < .004$) and tended to be lower for the verbal task than for the shape-color one ($p = .056$), while it did not differ between the verbal and the spatial tasks ($p = .22$). Moreover, in the repeat condition, accuracy was lower in the verbal and spatial tasks than in the shape-color task (for both, $Z > 3.15$, $p < .01$), but it was not different between verbal and spatial tasks ($p = .75$). In the switch condition, the accuracy level was lower for the verbal and spatial tasks than for the shape-color one (for both, $Z > 3.2$, $p < .01$), but again it did not differ between the verbal and spatial tasks ($p = .64$).

Shape-color mixing cost and FA/RD correlations

The regression analysis determined that the shape-color mixing cost is negatively related to FA and RD in 1178 voxels, divided into three clusters. The biggest cluster, having its global maximum located in the superior corona radiata [24, −14, 32, in MNI space coordinates], contained 957 voxels and spanned on portions of the posterior and superior corona radiata (right side only) extending from the body of corpus callosum. Up to six local maxima could be identified within this cluster. The second cluster, containing 194 voxels, was located across portions of anterior corona radiata (left only), stemming from the genu of corpus callosum. The peak voxel was located in the genu of corpus callosum [−6, 31, 6], but this cluster counted up to five local maxima. The third cluster was composed of 27 voxels and was located in the posterior corona radiata (left side only). This cluster showed two local maxima beside the global maximum, which is located in [−26, −33, 27]. Figs. 1–3 show the regression plot of significant negative correlations between shape-color mixing costs and FA for each cluster and their position (thickened) on the mean FA image, while Table 2 shows the correlation coefficients found in all the local and global maxima.

Spatial mixing cost and FA/RD correlations

The regression analysis showed that the spatial mixing cost was negatively associated with FA and RD in 4487 voxels, all being part of a unique cluster located across portions of anterior corona radiata (bilateral, but mostly right), superior corona radiata (bilateral), posterior corona radiata (left only), genu, body and splenium of corpus callosum. This cluster showed its global maximum in the genu of corpus callosum [−11, 26, 16, in MNI space coordinates], although it comprised six different local maxima. Fig. 4 shows the regression plot of significant negative correlation between spatial mixing costs and FA in the voxel corresponding to the peak statistics. Table 3 shows the correlation coefficients found in the global maximum and all the six local maxima.

Verbal mixing cost and FA/RD correlations

The regression analysis showed that verbal mixing cost was not related to either FA or RD, when a similar statistical approach to correct for multiple comparisons was applied. Therefore, this index was discarded from further analyses.

Conjunction analysis

This analysis determined that both spatial and shape-color mixing costs were related to FA and RD in 220 voxels, divided into eight clusters. Only two of them however contained more than 10 voxels.

The first cluster contained 118 voxels, and spanned on portions of the anterior corona radiata, left side only, extending from the genu of corpus callosum. It had its maximum in the genu of corpus callosum [−11, 33, 7], although up to three local maxima could be identified within this cluster. The second cluster, containing 71 voxels, was located across portions of superior corona radiata (right only), stemming from the body of corpus callosum. The peak statistical value was located in the body of corpus callosum [18, −7, 39], but this cluster counted up to four local maxima. Fig. 5 shows each of these two clusters. Table 4 shows the correlation coefficients found in all the local and global maxima.

DISCUSSION

The goal of the present study was to characterize how WM structural integrity may support high-level executive

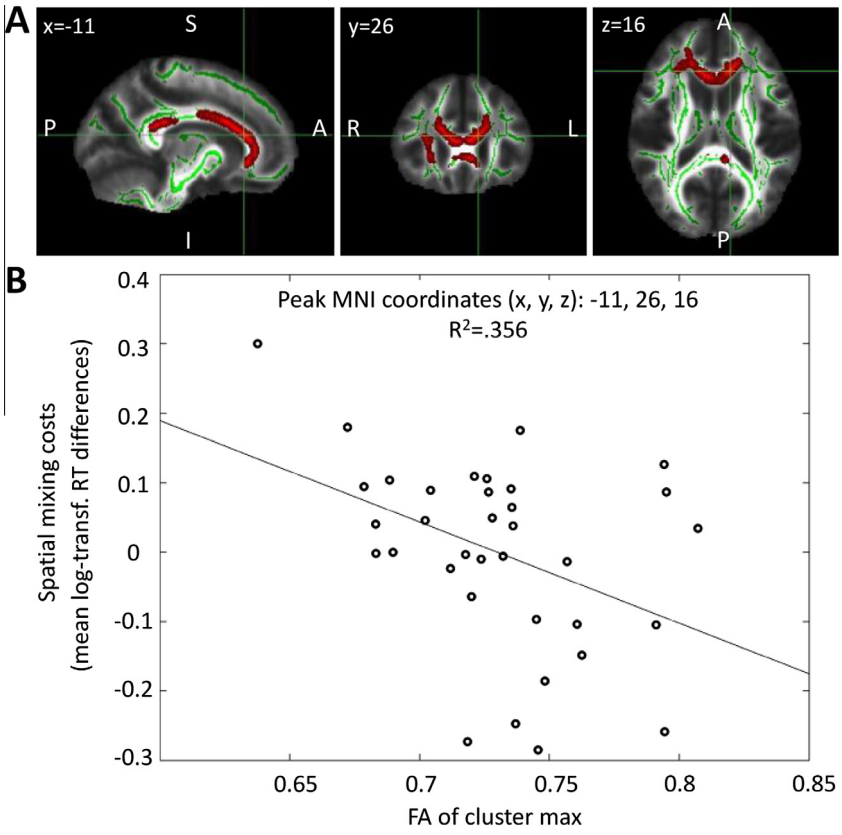

Fig. 1. Relationship between fractional anisotropy (FA), radial diffusivity (RD) and the mixing cost performance in the shape-color task in the voxel corresponding to the peak statistics of the largest cluster (containing 957 voxels). (A) The cluster colored in a red scale contains overlapping voxels showing significant correlations both between FA and mixing costs and between RD and mixing costs. Higher FA and lower RD in the highlighted cluster are associated with better performance. The cluster is overlaid on mean white matter skeleton, shown in green. All images are displayed in radiological convention. The cluster is significant at a voxel-wise $p < 0.05$, corrected for multiple comparisons using TFCE. Coordinates are presented in MNI space. L and R stand for left and right, respectively; P and A stand for posterior and Anterior; S and I stand for superior and inferior. (B) Graph showing the correlation between higher FA in the cluster and shape-color mixing costs in the voxel corresponding to the peak statistics. (For interpretation of the references to color in this figure legend, the reader is referred to the web version of this article.)

functions required in different task-switching paradigms. In particular, we aimed at finding WM correlates of performance according to the specific rules used in three different task-switching paradigms.

Behaviorally, all the three task-switching paradigms produced reliable switching and mixing costs, although they showed different general difficulty levels, with RTs for the verbal tasks being the longest and those for the shape-color tasks being the shortest. These differences were seen particularly in single task blocks, while they diminished considerably in mixing contexts. To account for these results, we could speculate that, while the two verbal task pairs and the two spatial ones involved qualitatively akin rules processed by similar neuronal substrates (grammatical and rotational, respectively), the third paradigm involved color and shape judgments, which are known to be separately processed in lower level visual cortices and could be integrated (and possibly differently weighted when they compete for response execution) only in higher level V4/infero-temporal regions (e.g., Hubel and Wiesel, 2005), thus increasing processing times (and RTs) in mixing vs. single-task blocks. Above and beyond all the differences in terms of both experimental design and behavioral effects, the overarching goal of the present study was to detect common WM tracts underpinning performance in mixing task-switching blocks in different tasks and stimulus domains.

It is interesting to note that domain-specific correlations between behavior and posterior WM tracts, located in the posterior corona radiata in both non-verbal tasks and the splenium in the spatial task, which were present for the two non-verbal tasks, disappeared in the conjunction analysis. On the other hand, clusters in the genu and body of corpus callosum survived the conjunction analysis. These results suggest that the microstructure of inter-hemispheric connections in more anterior regions of the brain (particularly, the genu of corpus callosum), is more likely to explain behavioral performance in a domain-general fashion, especially for more complex and difficult task conditions (Davis and Cabeza, 2015). More generally, our results support the idea that frontal regions have a task-general role in performing demanding cognitive tasks (Velanova et al., 2007; McGilchrist, 2010; Davis and Cabeza, 2015; Yeo et al., 2015).

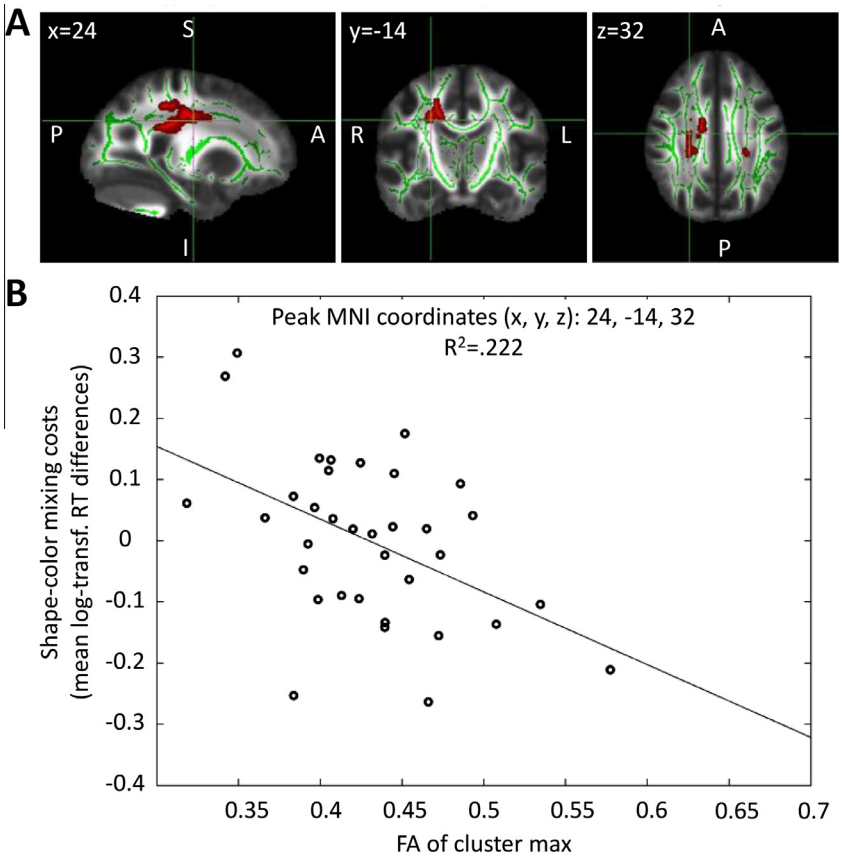

Fig. 2. Relationship between fractional anisotropy (FA), radial diffusivity (RD) and the mixing cost performance in the shape-color task in the voxel corresponding to the peak statistics of the medium-sized cluster (containing 194 voxels). (A) The colored cluster contains overlapping voxels showing significant correlations both between FA and mixing costs and between RD and mixing costs. Higher FA and lower RD in the highlighted cluster are associated with better performance. (B) Graph showing the correlation between higher FA in the cluster and shape-color mixing costs in the voxel corresponding to the peak statistics. See Fig. 1 for all the other details. (For interpretation of the references to color in this figure legend, the reader is referred to the web version of this article.)

However, since we did not find these results with a purely verbal (grammatical) version of the task-switching paradigm (also see Gold et al., 2010, for similar null results on another verbal version of the task-switching paradigm in young individuals), we may speculate that a critical factor to be considered as an account for our results is the non-verbal components of the two tasks included in the conjunction analysis. Although both the spatial and shape-color tasks may involve some verbal demands and strategies, they also embed rules with non-verbal perceptual features (concerning space, shape, and color). These two tasks might require better connectivity between the two frontal lobes, when task-switching is considered, thus explaining the location of the global maxima in the anterior parts of the corpus callosum. Indeed previous fMRI evidence (Vallesi et al., 2015) showed that, while a left fronto-parietal network is involved in mixing blocks for purely verbal tasks, a homologous region in the right prefrontal cortex was additionally recruited when performing a spatial version of the task.

Caution should be applied when interpreting the null result concerning the verbal task, which was also the most challenging in terms of absolute RTs. Accounts regarding differences in the difficulty level could not be discarded, although two considerations reduce their plausibility. First, the accuracy level was not different from that of the spatial task, which was equally less accurate with respect to the shape-color one but showed significant results. Moreover, the RT mixing costs, a measure of difficulty in the specific processes involved during the task-switching blocks, were intermediate in the verbal task, which showed null effects, with respect to those in the other two tasks, which instead showed significant correlations with WM microstructural characteristics.

We also had the chance to run the same correlation analyses between DTI and the verbal task-switching performance on a subset of participants (29/35) who performed a similar task during an fMRI session (see Vallesi et al., 2015). Again, we could not find any significant correlation between verbal mixing costs and DTI measures, which increased our confidence toward the genuineness of the reported null result, although this outcome is not surprising given the slightly lower sample size and the less than ideal conditions produced by the scanner environment (Hommel et al., 2012) and fMRI-oriented adjustments to the task-switching paradigms (Ruge et al., 2013).

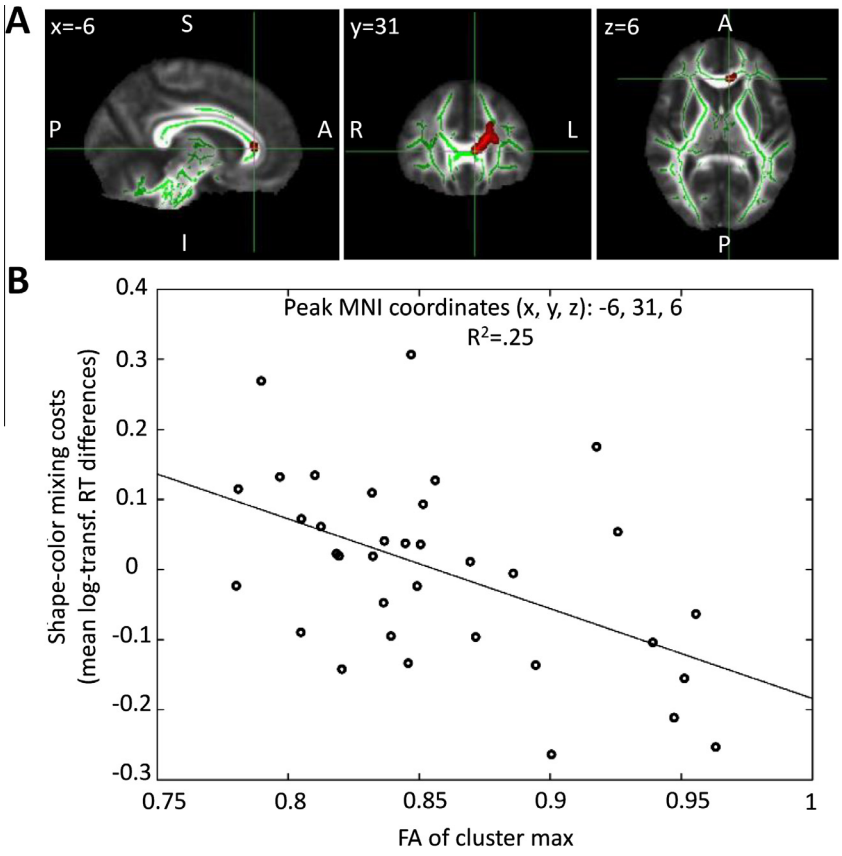

Fig. 3. Relationship between fractional anisotropy (FA), radial diffusivity (RD) and the mixing cost performance in the shape-color task in the voxel corresponding to the peak statistics of the smallest cluster (containing 27 voxels). (A) The cluster colored in a red scale contains overlapping voxels showing significant correlations both between FA and mixing costs and between RD and mixing costs. Higher FA and lower RD in the highlighted cluster are associated with better performance. (B) Graph showing the correlation between higher FA in the cluster and shape-color mixing costs in the voxel corresponding to the peak statistics. See Fig. 1 for all the other details. (For interpretation of the references to color in this figure legend, the reader is referred to the web version of this article.)

Thus, although it is always difficult to deal with a null result, the fact that the integrity of WM was not associated with performance on the grammatical version of the task-switching paradigm could partially and very cautiously be interpreted as due to heavy left hemispheric specialization for language functions (Seghier and Price, 2011; Hervé et al., 2013) and a poor role of inter-hemispheric connectivity for verbal material, at least in young adulthood (cf., Cabeza et al., 1997; Perani et al., 2011), when connectivity in general is conceivably close to ceiling. Similar trends are observed with right-hemispheric basic visuo-spatial functions (Everts et al., 2009; Groen et al., 2012). However, even this domain-specific account does not fully explain why, in a performance measure specifically linked to right prefrontal functionality such as the mixing costs (e.g., Braver et al., 2003; also see Ambrosini and Vallesi, 2016), a relation with WM microstructure in inter-hemispheric connections did not emerge when the (verbal) material is processed in the left hemisphere while the critical processes (sustained task-switching control) occur in the right one. Future investigation should further test the WM role in task-switching with different task contexts, also using different versions of the verbal task-switching paradigm, to try to exclude other possible task-specific idiosyncrasies such as differences in general difficulty.

The association between lower mixing costs and higher WM integrity in the body of corpus callosum/superior corona radiata, in the territory underneath the pre-central cortex, which also emerged in the conjunction analysis, replicates and extends previous findings by Seghete and colleagues (2013), who also found similar effects in adolescents, independently of age. These findings highlight a role of motor/premotor connections in sustaining task-switching performance, probably due to the importance of these regions in implementing stimulus–response associations during task-switching blocks.

Using specific measures of task-switching performance, rather than a global switching cost (cf., Gold et al., 2010; Seghete et al., 2013), we were able, in principle, to look at the role of WM connectivity separately for phasic sub-processes with local switch costs and tonic ones with classical mixing costs during task-switching. However, preliminary analyses did not show associations between WM integrity and switch costs that would survive the chosen statistical threshold. It is interesting to note that none of the previous DTI works reported WM correlates of pure switch costs: two studies failed to report these correlates because they did not adopt this measure (Gold et al., 2010; Seghete et al., 2013), and one because it obtained a null result on

Table 2. Correlation coefficients found in the global maxima and the local maxima between fractional anisotropy (FA) and the shape-color mixing cost (all coefficients are negative). Maximum identifier, MNI coordinates, predicted structure/tract the voxel belongs to and coefficient of determination for the linear fit. The FA results presented in this table were masked with those of the equivalent correlation analysis with radial diffusivity, and thus represent regions of common significant effects (although the correlation coefficients had opposite directions: negative for FA and positive for RD). CR = corona radiata, CC = corpus callosum, R = right, L = left

	Position (MNI space)	Structure	Tract (> 10% probability)	*R*	R^2 (*p*-value)
Global Maximum (957 voxels)	[24, −14, 32]	Superior CR-R	24% Corticospinal tract R	−.471	.222 (.0132)
Local Max 1	[19, −11, 43]	Superior CR-R	–	−.477	.228
Local Max 2	[19, −9, 42]	Superior CR-R	–	−.507	.257
Local Max 3	[21, −37, 41]	Unclassified	–	−.506	.256
Local Max 4	[18, −9, 40]	Superior CR-R	–	−.461	.213
Local Max 5	[18, −7, 39]	Superior CR-R	–	−450	.203
Local Max 6	[19, −16, 39]	Superior CR-R	–	−.445	.198
Global Maximum (194 voxels)	[−6, 31, 6]	Genu CC	79% Forceps minor	−.500	.250 (.0158)
Local Max 1	[−20, 31, 14]	Anterior CR-L	37% Anterior thalamic radiation L, 11% Inferior fronto-occipital fasciculus L	−.423	.179
Local Max 2	[−22, 32, 13]	Anterior CR-L	55% Anterior thalamic radiation L	−.386	.149
Local Max 3	[−22, 30, 13]	Anterior CR-L	58% Anterior thalamic radiation L, 11% Inferior fronto-occipital fasciculus L	−.390	.152
Local Max 4	[−9, 28, 12]	Genu CC	63% Forceps minor	−.392	.154
Local Max 5	[−6, 31, 6]	Genu CC	79% Forceps minor	−.500	. 250
Global Maximum (27 voxels)	[−26, −33, 27]	Posterior CR-L	–	−.608	.370 (.0154)
Local Max 1	[−22, −32, 29]	Unclassified	–	−.591	.349
Local Max 2	[−26, −33, 27]	Posterior CR-L	–	−.608	.370

children (Treit et al., 2014). There are several potential explanations for this repeatedly reported null result (and corresponding lack of reported significant results). For instance, one could postulate that, since the time-scale in which switch costs emerge is much smaller than that for mixing costs, which makes the former a marker of much more phasic processes, it is possible that (time-consuming) inter-regional connectivity is less fundamental in this case. Another possible reason is the fact that similar brain regions (and their underlying connectivity) are involved in both switch and repeat trials, even if to a different level, especially with equal probability of occurrence (e.g., Dove et al., 2000; see Ruge et al., 2013, for a review), thus explaining the low anatomical sensitivity of a performance index that differentiates between these two conditions (local switch costs). These are post hoc explanations and further investigation is necessary, possibly with a higher number of participants to completely exclude power issues.

Unlike a previous DTI study (Gold et al., 2010), we did not find associations between the superior longitudinal fasciculus and task-switching performance. The lack of this effect is somewhat surprising, since this big tract is supposed to connect nodes of the fronto-parietal network which previous fMRI studies found to be involved in task-switching (see Kim et al., 2012; Jamadar et al., 2015, for meta-analyses). Apart from the reported whole-brain analysis, as an internal check, we also performed a ROI analysis on the superior longitudinal fasciculus (as in Gold et al., 2010), which confirmed the result of the whole-brain approach, that is, no correlation between the DTI derived indices and the task-switching-related ones.

We cannot simply attribute our failure to replicate previous findings to lack of power, since Gold and colleagues' (2010) study involved almost half of our participants in their young group ($N = 20$) and we had the chance to search for a significant association between behavioral task-switching measures and DTI indices in the superior longitudinal fasciculus, if it existed, in three different task-switching versions. However, the absence of this association resembles the results of another previous DTI study (Seghete et al., 2013). Future work should investigate which task- and sample-specific features might explain these discrepancies.

Notwithstanding the several advantages offered by the methodology employed in the present study, primarily the possibility to run group-level whole-brain analyses within a common WM template, there are also some limitations inherent to it. First of all, FA and RD are both indirect measures of WM anisotropy properties and, although they represent some of the currently best available proxies, these measures might be influenced by several factors other than microstructural anisotropy and orientation of axons. Besides, it has to be kept in mind that regions showing multiple crossing fibers can reduce FA, therefore challenging result interpretation. Indeed the diffusion tensor model fails to detect a main diffusion direction in those areas, thus leading to lower FA values estimation. Moreover, each estimate is limited by inherent noise of the MR acquisition process and possible partial volume effects.

One last issue needs to be discussed. Voxel-based analysis requires both normalization to a template and skeletonization, two steps which allow generalization

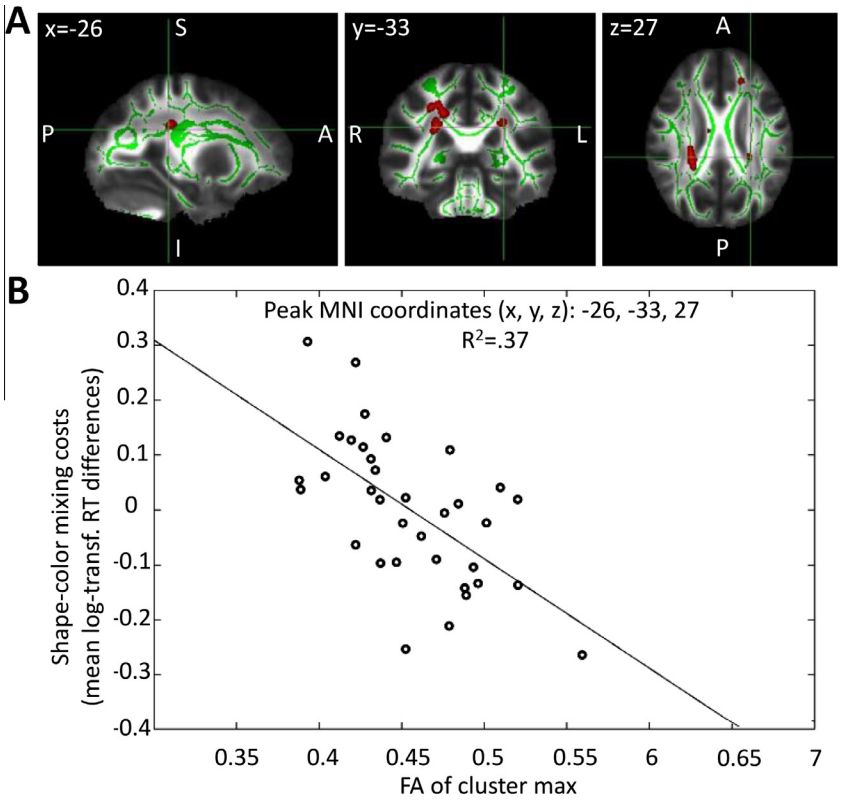

Fig. 4. Relationship between fractional anisotropy (FA), radial diffusivity (RD) and the mixing cost performance in the spatial task. (A) The cluster displayed in red contains the overlapping voxels that show significant correlations both between FA and mixing costs and between RD and mixing costs. Higher FA and lower RD in the highlighted cluster are associated with better performance. The cluster (containing 4487 voxel) is overlaid on mean white matter skeleton, shown in green. (B) Graph showing the correlation between higher FA in the cluster and spatial mixing costs in the voxel corresponding to the peak statistics. See Fig. 1 for all the other details. (For interpretation of the references to color in this figure legend, the reader is referred to the web version of this article.)

Table 3. Correlation coefficients found in the global maximum and the six local maxima between fractional anisotropy (FA) and the spatial mixing cost. Maximum identifier, MNI coordinates, predicted structure/tract the voxel belongs to and coefficient of determination for the linear fit. The FA results presented in this table were masked with those of the equivalent correlation analysis with radial diffusivity (RD), and thus represent regions of common significant effects (although the correlation coefficients had opposite directions: negative for FA and positive for RD). CR = corona radiata, CC = corpus callosum, R = right, L = left

	Position (MNI space)	Structure	Tract (>10% probability)	*R*	R^2 (*p*-value)
Global Maximum (4487 voxels)	[−11, 26, 16]	Genu CC-L	42% Forceps minor	−.597	.356 (.00659)
Local Max 1	[−16, 29, 22]	Anterior CR-L	11% Cingulate gyrus L	−.563	.317
Local Max 2	[−14, 28, 17]	Genu CC-L	42% Forceps minor	−.581	.338
Local Max 3	[−13, 30, 16]	Genu CC-L	47% Forceps minor, 14% Cingulate gyrus L	−.553	.306
Local Max 4	[−11, 26, 16]	Genu CC-L	42% Forceps minor	−.597	.356
Local Max 5	[−14, 18, 24]	Body CC-L	–	−.491	.241
Local Max 6	[−17, 25, 22]	Genu CC-L	–	−.493	.243

across individuals, but at the cost of introducing some possible registration errors and loss of individually-specific information. Thus, it is reasonable to state that the picture offered by the present approach may represent only a partial story and other higher-spatial resolution tractographic approaches might be more useful to do inter-individual differences justice especially for the minor tracts that were neglected in the present study. Related to the latter issue, it is to note that deterministic tractography has some limits. Noise and partial volume effects in diffusion tensor estimate can cause an early interruption of the tracts due to, for example, regions with crossing fibers (e.g., Jeurissen et al., 2013), as already stated. This might partially explain why some of the identified local maxima cannot be annotated by means of the JHU WM tractography atlas.

As a final related note, even if the main results concerned anterior inter-hemispheric regions that are most likely attributable to corpus callosum forceps minor, there was also evidence, particularly for the shape-color paradigm, for a role of intra-hemispheric

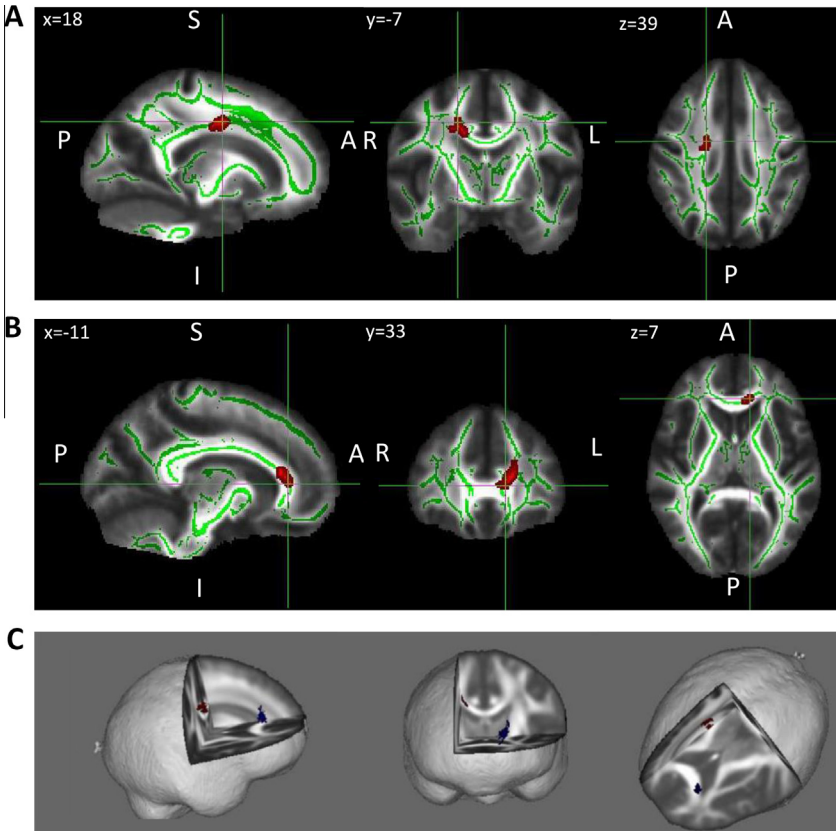

Fig. 5. The two clusters of voxels showing a significant relationship between fractional anisotropy (FA), radial diffusivity (RD) and the mixing cost performance in both the shape-color and the spatial paradigm (conjunction analysis). The two clusters containing 118 and 71 voxels, respectively, are represented in (A) and (B), with a 3D view of both clusters (in blue and red) in (C). See Fig. 1 for all the other details. (For interpretation of the references to color in this figure legend, the reader is referred to the web version of this article.)

Table 4. Correlation coefficients found in the global maxima and the local maxima between fractional anisotropy (FA) and the overall mixing cost resulting from conjunction analysis on spatial and shape-color task-switching paradigms (MxSpa and MxCS, respectively). Maximum identifier, MNI coordinates, predicted structure/tract the voxel belongs to and coefficient of determination for the linear fit. The FA results presented in this table were masked with those of the equivalent correlation analysis with radial diffusivity (RD), and thus represent regions of common significant effects. CR = corona radiata, CC = corpus callosum, R = right, L = left

	Position (MNI space)	Structure	Tract (> 10% probability)	R^2 (p-value) FA-MxSpa	R^2 (p-value) FA-MxCS
Global Maximum (118 voxels)	[−11, 33, 7]	Genu CC-L	71% Forceps minor, 11% Cingulate gyrus L	.071 (< .01)	.198 (< .05)
Local Max 1	[−9, 28, 12]	Genu CC-L	63% Forceps minor	.1699	.154
Local Max 2	[−10, 31, 11]	Genu CC-L	63% Forceps minor, 11% Cingulate gyrus L	.098	.153
Local Max 3	[−11, 33, 7]	Genu CC-L	71% Forceps minor, 11% Cingulate gyrus L	.071	.198
Global Maximum (71 voxels)	[18, −7, 39]	Superior CR-R	–	.085 (< .05)	.203 (< .05)
Local Max 1	[18, −14, 36]	Body CC-R	–	.0857	.176
Local Max 2	[17, −10, 37]	Superior CR-R	–	.191	.116
Local Max 3	[14, −12, 33]	Body CC-R	–	.163	.139
Local Max 4	[14, −10, 32]	Body CC-R	–	.115	.185

WM tracts, such as left anterior thalamic radiation and right cortico-spinal tract. As already stated, future directions should include finer grained tractography analyses, possibly on DTI data with a higher number of gradients than the 32 directions employed in the present dataset, in order to allow stronger spatial inferences about connectivity.

CONCLUSION

The present findings show that maintaining and managing different task rules during task-switching blocks benefit from a more efficient WM connectivity through portions of the corpus callosum connecting the two frontal lobes, at least when the rules entail non-verbal demands,

highlighting the importance of anterior inter-hemispheric connectivity for this key capacity at the basis of cognitive flexibility. Future work adopting different approaches should investigate the specific (excitatory or inhibitory) nature of these frontal inter-hemispheric interactions underpinning the flexible regulation of behavior in more detail.

Acknowledgments—This work was funded by the European Research Council Starting Grant LEX-MEA GA n° 313692 (FP7/2007-2013) to AV. The authors thank Mariagrazia Capizzi, Sandra Arbula and Ettore Ambrosini, for help in data collection and preliminary analysis, Marco Castellaro for his assistance in setting up DTI sequences, and the Città della Speranza Foundation in Padova, for its logistic support.

REFERENCES

Alexander AL, Hurley SA, Samsonov AA, Adluru N, Hosseinbor AP, Mossahebi P, Tromp Do PM, Zakszewski E, Field AS (2012) Characterization of cerebral white matter properties using quantitative magnetic resonance imaging stains. Brain Connect 1(6):423–446.

Alexander AL, Lee JE, Lazar M, Field AS (2007) Diffusion tensor imaging of the brain. Neurotherapeutics 4(3):316–329.

Ambrosini E, Vallesi A (2016) Asymmetry in prefrontal resting-state EEG spectral power underlies individual differences in phasic and sustained cognitive control. Neuroimage 124(1):843–857.

Andersson JLR, Jenkinson M, Smith S (2007a) TR07JA1: Non-linear optimisation, FMRIB Technical Report, 2007.

Andersson JLR, Jenkinson M, Smith S (2007b) TR07JA2: Non-linear registration, aka Spatial normalisation, 2007.

Babcock L, Vallesi A (2015) The interaction of process and domain in prefrontal cortex during inductive reasoning. Neuropsychologia 67:91–99.

Badre D, Wagner AD (2006) Computational and neurobiological mechanisms underlying cognitive flexibility. Proc Natl Acad Sci U S A 103(18):7186–7191.

Basser PJ, Pierpaoli C (1996) Microstructural and physiological features of tissues elucidated by quantitative-diffusion-tensor MRI. J Magn Reson Ser B 111(3):209–219.

Beaulieu C (2002) The basis of anisotropic water diffusion in the nervous system - a technical review. NMR Biomed 15(7–8):435–455.

Boekel W, Wagenmakers E-J, Belay L, Verhagen J, Brown S, Forstmann BU (2015) A purely confirmatory replication study of structural brain-behavior correlations. Cortex 66:115–133.

Brass M, von Cramon DY (2004) Decomposing components of task preparation with functional magnetic resonance imaging. J Cognitive Neurosci 16(4):609–620.

Braver TS, Reynolds JR, Donaldson DI (2003) Neural mechanisms of transient and sustained cognitive control during task switching. Neuron 39(4):713–726.

Cabeza R, McIntosh AR, Tulving E, Nyberg L, Grady CL (1997) Age-related differences in effective neural connectivity during encoding and recall. NeuroReport 8(16):3479–3483.

Cohen J (1977) Statistical power analysis for the behavioral sciences. New York, NY: Academic Press.

Crone EA, Wendelken C, Donohue SE, Bunge SA (2006) Neural evidence for dissociable components of task-switching. Cereb Cortex 16:475–486.

Davis SW, Cabeza R (2015) Cross-hemispheric collaboration and segregation associated with task difficulty as revealed by structural and functional connectivity. J Neurosci 35 (21):8191–8200.

De Baene W, Kühn S, Brass M (2012) Challenging a decade of brain research on task switching: Brain activation in the task-switching paradigm reflects adaptation rather than reconfiguration of task sets. Hum Brain Mapp 33:639–651.

Dove A, Pollmann S, Schubert T, Wiggins CJ, von Cramon DY (2000) Prefrontal cortex activation in task switching: an event-related fMRI study. Brain Res Cogn Brain Res 9(1):103–109.

Everts R, Lidzba K, Wilke M, Kiefer C, Mordasini M, Schroth G, Perrig W, Steinlin M (2009) Strengthening of laterality of verbal and visuospatial functions during childhood and adolescence. Hum Brain Mapp 30(2):473–483.

Feldman HM, Yeatman JD, Lee ES, Barde LH, Gaman-Bean S (2010) Diffusion tensor imaging: A review for pediatric researchers and clinicians. J Dev Behav Pediatr 31(4):346–356.

Gold BT, Powell DK, Xuan L, Jicha GA, Smith CD (2010) Age-related slowing of task switching is associated with decreased integrity of frontoparietal white matter. Neurobiol Aging 31(3):512–522.

Groen MA, Whitehouse AJO, Badcock NA, Bishop DVM (2012) Does cerebral lateralization develop? A study using functional transcranial Doppler ultrasound assessing lateralization for language production and visuospatial memory. Brain Behav 2 (3):256–269.

Hervé P-Y, Zago L, Petit L, Mazoyer B, Tzourio-Mazoyer N (2013) Revisiting human hemispheric specialization with neuroimaging. Trends Cogn Sci 17(2):69–80.

Hommel B, Fischer R, Colzato LS, van den Wildenberg WPM, Cellini C (2012) The effect of fMRI (noise) on cognitive control. J Exp Psychol Hum 38(2):290–301.

Hubel DH, Wiesel TN (2005) Brain and visual perception. New York: Oxford Press.

Jamadar SD, Thienel R, Karayanidis F (2015) Task switching processes. In: Brain mapping: An encyclopedic reference. p. 327–335.

Jeurissen B, Leemans A, Tournier J-D, Jones DK, Sijbers J (2013) Investigating the prevalence of complex fiber configurations in white matter tissue with diffusion magnetic resonance imaging. Hum Brain Mapp 34:2747–2766.

Kim C, Cilles SE, Johnson NF, Gold BT (2012) Domain general and domain preferential brain regions associated with different types of task switching: a meta-analysis. Hum Brain Mapp 33 (1):130–142.

Kim C, Johnson NF, Cilles SE, Gold BT (2011) Common and distinct mechanisms of cognitive flexibility in prefrontal cortex. J Neurosci 31(13):4771–4779.

Le Bihan D (2003) Looking into the functional architecture of the brain with diffusion MRI. Nat Rev Neurosci 4(6):469–480.

McGilchrist I (2010) Reciprocal organization of the cerebral hemispheres. Dialogues Clin Neurosci 12(4):503–515.

Miyake A, Friedman NP, Emerson MJ, Witzki AH, Howerter A, Wager TD (2000) The unity and diversity of executive functions and their contributions to complex "Frontal Lobe" tasks: a latent variable analysis. Cogn Psychol 41(1):49–100.

Oldfield RC (1971) The assessment and analysis of handedness: The Edinburgh inventory. Neuropsychologia 9:97–113.

O'Sullivan M, Jones DK, Summers PE, Morris RG, Williams SC, Markus HS (2001) Evidence for cortical "disconnection" as a mechanism of age-related cognitive decline. Neurology 57 (4):632–638.

Perani D, Saccuman MC, Scifo P, Anwander A, Awander A, Spada D, Baldoli C, Poloniato A, Lohmann G, Friederici AD (2011) Neural language networks at birth. Proc Natl Acad Sci U S A 108 (38):16056–16061.

Pfefferbaum A, Sullivan EV, Hedehus M, Lim KO, Adalsteinsson E, Moseley M (2000) Age-related decline in brain white matter anisotropy measured with spatially corrected echo-planar diffusion tensor imaging. Magn Reson Med 44(2):259–268.

Rogers RD, Monsell S (1995) Costs of a predictable switch between simple cognitive tasks. J Exp Psychol Gen 124(2):207–231.

Rousseeuw PJ, Verboven S (2002) Robust estimation in very small samples. Comput Stat Data Anal 40(4):741–758.

Rubin O, Meiran N (2005) On the origins of the task mixing cost in the cuing task-switching paradigm. J Exp Psychol Learn 31 (6):1477–1491.

Rueckert D, Sonoda LI, Hayes C, Hill DLG, Leach MO, Hawkes DJ (1999) Nonrigid registration using free-form deformations: Application to breast MR images. IEEE Trans Med Imaging 18 (8):712–721.

Ruge H, Jamadar S, Zimmermann U, Karayanidis F (2013) The many faces of preparatory control in task switching: Reviewing a decade of fMRI research. Hum Brain Mapp 34:12–35.

Seghete KLM, Herting MM, Nagel BJ (2013) White matter microstructure correlates of inhibition and task-switching in adolescents. Brain Res 1527:15–28.

Seghier ML, Price CJ (2011) Explaining left lateralization for words in the ventral occipitotemporal cortex. J Neurosci 31 (41):14745–14753.

Smith SM (2002) Fast robust automated brain extraction. Hum Brain Mapp 17(3):143–155.

Smith SM, Jenkinson M, Johansen-Berg H, Rueckert D, Nichols TE, Mackay CE, Watkins KE, Ciccarelli O, Cader MZ, Matthews PM, Behrens TEJ (2006) Tract-based spatial statistics: voxelwise analysis of multi-subject diffusion data. Neuroimage 31 (4):1487–1505.

Smith SM, Nichols TE (2009) Threshold-free cluster enhancement: addressing problems of smoothing, threshold dependence and localisation in cluster inference. Neuroimage 44(1):83–98.

Treit S, Chen Z, Rasmussen C, Beaulieu C (2014) White matter correlates of cognitive inhibition during development: a diffusion tensor imaging study. Neuroscience 276:87–97.

Vallesi A, Arbula S, Capizzi M, Causin F, D'Avella D (2015) Domain-independent neural underpinning of task-switching: an fMRI investigation. Cortex 65:173–183.

Velanova K, Lustig C, Jacoby LL, Buckner RL (2007) Evidence for frontally mediated controlled processing differences in older adults. Cereb Cortex 17(5):1033–1046.

Verboven S, Hubert M (2010) MATLAB library LIBRA. Wiley Interdiscip Rev Comput Stat 2(4):509–515.

Wang Y, Kuhl PK, Chen C, Dong Q (2009) Sustained and transient language control in the bilingual brain. Neuroimage 47(1):414–422.

Wylie GR, Murray MM, Javitt DC, Foxe JJ (2009) Distinct neurophysiological mechanisms mediate mixing costs and switch costs. J Cogn Neurosci 21(1):105–118.

Yeo BTT, Krienen FM, Eickhoff SB, Yaakub SN, Fox PT, Buckner RL, Asplund CL, Chee MW (2015) Functional specialization and flexibility in human association cortex. Cereb Cortex 25:3654–3672.

Zhu Z, Hakun JG, Johnson NF, Gold BT (2014) Age-related increases in right frontal activation during task switching are mediated by reaction time and white matter microstructure. Neuroscience 278:51–61.

(Accepted 12 May 2016)
(Available online 20 May 2016)